

## z-Pinch Plasma Lens Focusing of a Heavy-Ion Beam

E. Boggasch, J. Jacoby, and H. Wahl

*Max-Planck-Institut für Quantenoptik (MPQ), D-8046 Garching, Federal Republic of Germany*

K.-G. Dietrich, D. H. H. Hoffmann, and W. Laux

*Gesellschaft für Schwerionenforschung (GSI), D-6100 Darmstadt, Federal Republic of Germany*

M. Elfers and C. R. Haas

*Lehrstuhl für Lasertechnik, Rheinisch-Westfälische Technische Hochschule Aachen,  
D-5100 Aachen, Federal Republic of Germany*

V. P. Dubenkov and A. A. Golubev

*Institute for Theoretical and Experimental Physics, 117259 Moscow, U.S.S.R.*

(Received 6 December 1990)

For the first time a heavy-ion beam was focused using a z-pinch plasma lens. The diameter of an incident, parallel, 460-MeV argon-ion beam was reduced from  $\sim 8$  mm (FWHM) to  $\sim 2$  mm within 230 mm downstream of the plasma. Inside a cylindrically symmetric plasma column a high-gradient, azimuthal magnetic field is produced during a z-pinch discharge. For axially moving, high-energy charged particles this field configuration provides strong, first-order focusing simultaneously in both transversal planes. The measured spot size agrees with numerical calculations taking into account the finite beam emittance, and charge exchange as well as energy-loss processes contributing to aberrations.

PACS numbers: 52.55.Ez, 41.80.-y, 52.75.-d

Focusing of high-energy charged-particle beams is a crucial problem relevant for special applications in accelerator physics. Strong magnetic lenses with high focusing power are required to handle high-energy beams with large divergence. This may be, for example, at the final focus point where the beam cross section has to be reduced to a small spot size, or behind a production target where secondary diverging particles are to be captured. Quadrupole performance is limited when extreme symmetric focusing is required and both a high focusing gradient and a large aperture is needed at the same time. In the focusing plane the focal length  $f$  can be expressed as  $f = l / (\Phi \sin \Phi)$  for a lens of length  $l$  and with phase  $\Phi = \sqrt{\kappa} l$ , where  $\kappa$  is the focusing strength defined by  $\kappa = (Ze/p)G$ , with  $Z$  being the charge state,  $e$  the electron charge,  $p$  the particle momentum, and  $G$  the field gradient. For a phase  $\Phi < \pi/2$  the focal spot is placed behind the lens, separated by a drift space  $d = f \cos \Phi$ .

An ideal magnetic-field distribution with radially directed restoring forces proportional to the distance from the axis is realized inside a cylindrical conductor of radius  $r_p$  passed by an axial electric current  $I_p$  with a uniform current density ("wire lens"). The resulting azimuthal magnetic field  $B_\Phi$  varies linearly with radius  $r$  so that  $B_\Phi = \mu_0 I_p r / 2r_p^2 \pi$ , yielding a constant gradient  $G = B_\Phi / r = \mu_0 I_p / 2r_p^2 \pi$ . A wire lens exhibits strong, first-order focusing proportional to the azimuthal magnetic field, in contrary to a quadrupole multiplet where focusing is a net second-order effect. The particles to be focused by a wire lens have to penetrate the conducting lens matter. Absorption processes limit the choice and the length of the conducting lens material. Therefore this type of lens is of practical interest only for the focus-

ing of high-energy particles. Lithium was chosen as the lightest and least absorbing metal for the development of "lithium lenses."<sup>1,2</sup> A different and commonly used focusing device in accelerators is the "magnetic horn,"<sup>3</sup> which is a z-direction parabolically shaped metallic structure that is pulsed with a high current. Here the external magnetic field of the conductor is used for focusing.

Inside a conducting, current-carrying plasma column ("active" plasma lens) operating in a density regime below  $\sim 10^{19} \text{ cm}^{-3}$  absorption is almost negligible. In 1950, a 350-MeV  $p$  beam of the 184-in. cyclotron in Berkeley was focused for the first time by a plasma lens with moderate characteristics.<sup>4</sup> A stronger plasma lens with more focusing power was built in Brookhaven in 1964.<sup>5</sup> Here, a contracting plasma column generated during a dynamic 500-kA z-pinch discharge was used for capturing 3-GeV/c muons and kaons emerging as secondary particles from a target.

The concept of an active plasma lens was followed up again for a space-charge-compensated transport scheme of high-current light-ion beams guided in long, linear discharge channels ("z discharges");<sup>6-8</sup> however, z-pinch discharge modes have been avoided and have been identified as a possible source of instabilities. The experiments concentrated mainly on the channel transport of proton beams whereas ion-beam propagation and focusing have been studied only theoretically.<sup>9</sup>

A z-pinch plasma lens was also proposed as an effective collector lens for antiprotons at CERN. Extensive off-beam laboratory research has been conducted<sup>10,11</sup> which will permit a first operational in-beam testing of a plasma lens at the CERN antiproton target fa-

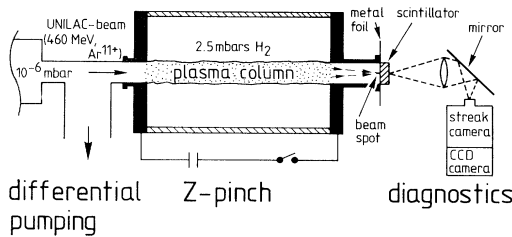


FIG. 1. Schematic representation of the focusing experiment.

cility, presumably in the near future.

At GSI, fundamental questions relevant for the physics of heavy-ion-beam-driven inertial-confinement-fusion research are being addressed. High-density, high-temperature plasmas are created by irradiating targets with heavy-ion beams.<sup>12</sup> Heavy ions yield a specific deposition power in matter which is proportional to the beam power and inversely proportional to the range of the ions and to the beam's spot size. In reducing the spot size by adding a plasma lens to the conventional quadrupole system, the achievable deposition power could be significantly enhanced.<sup>13</sup> In the course of the envisaged high-energy-density experiments at the new heavy-ion synchrotron facility SIS/ESR at GSI, a specific deposition power up to 10 TW/g is expected to be obtained in a target.<sup>14</sup>

In this Letter we report a first experiment which was performed to investigate the focusing behavior of a z-pinch plasma lens on a heavy-ion beam. The experimental setup is presented in Fig. 1 and the characteristics of the z-pinch discharge used are summarized in Table I. A parallel beam of 460 MeV (11.4 MeV/amu) of  $\text{Ar}^{11+}$  ions from the linear accelerator UNILAC at GSI propagated axially through the z-pinch quartz vessel filled with hydrogen gas of 2.5 mbar. The average electric particle current of the 500- $\mu\text{s}$ -long beam pulse was about 30  $\mu\text{A}$ . During the beam passage the discharge was triggered and a pinched plasma column of 20-mm diameter and 200-mm length was reproducibly formed along the axis within 1.3  $\mu\text{s}$  and remained optically stable for more than 500 ns. A 10-mm-wide aperture was provided along the entire experiment for the propagating beam to exclude beam interaction with solid windows. An efficient differential pumping system was installed to separate the gas pressure in the discharge vessel from the accelerator vacuum of less than  $10^{-6}$  mbar. The beam spot was observed downstream of the plasma using a fast plastic scintillator which was positioned at 230 and 380 mm behind the pinch. The emitted scintillator light was monitored using fast streak and framing photography. The streak images were registered by a charge-coupled-device (CCD) camera system for further numerical image processing, while the framing images were registered on photographic film. The side of the scintillator facing the plasma was covered by a 20- $\mu\text{m}$ -thick aluminum foil thus shielding the plasma light but still allowing the ions

TABLE I. Characteristic data of the z pinch.

Capacitance	4 $\mu\text{F}$
Charging voltage	32.5 kV
Inductance	15 nH
Current rise rate	$10^{12}$ A/s
Maximum current	400 kA
Filling gas	Hydrogen
Gas pressure	2.5 mbar
Length	200 mm
Tube radius	54 mm
Pinch radius	$\sim 10$ mm
Pinch plasma density	$1.5 \times 10^{19}$ $\text{cm}^{-3}$

to penetrate. The magnetic field was measured inductively using small coils<sup>15</sup> inserted axially through the electrodes into the discharge volume. Up to now magnetic-field data have been taken only at radii equal to or larger than the pinch radius of 10 mm (Ref. 16) due to difficulties related to the probing technique used.

A time-dependent overview of the experimental results is presented in Fig. 2. The wave forms of the discharge current and the magnetic field at the pinch radius are seen in Figs. 2(a) and 2(b), respectively. The field peaks at 1.6  $\mu\text{s}$  ("magnetic pinch time"), about 300 ns after the optically visible pinching starts. A time-correlated streak image of the beam spot diameter on the scintillator taken at a distance of 380 mm behind the pinch is shown in Fig. 2(c). The spot size shrinks during the discharge. Slight variations of intensity before and after the contraction are caused by fluctuations of the ion source current. A small misalignment of the pinch axis from the beam axis leads to a slightly off centered but reproducible contraction. Figure 2(d) shows a series of end-on framing pictures of the entire beam spot, also taken at 380 mm distance. The maximum focusing, witnessed at 380 mm after  $\sim 1.3$   $\mu\text{s}$ , occurs while the magnetic field is still rising. As the magnetic-field amplitude is changing with time, the location of the focal spot behind the pinch is also time dependent. A constant magnetic-field gradient of 12 T/m is necessary to produce a focus at the chosen distance  $d$  of 380 mm behind the lens. At time of maximum field (1.6  $\mu\text{s}$ ) the spot diameter has increased again to about 5 mm because the gradient reaches 25 T/m, now producing the focal spot at  $d \approx 160$  mm. Thus, at 380 mm distance, the beam is overfocused at that time. Streak images taken at  $d = 230$  mm show that the spot size has been reduced approximately by a factor of 4 to about 2 mm (FWHM) from its initial value of 8 mm (FWHM) at the magnetic pinch time. Mechanical constraints did not allow us to place the scintillator at the shortest focal length of 160 mm.

The focusing occurs although the discharge current is small and close to the zero crossing of the signal. The axially measured magnetic field in Fig. 2(b), causing the focusing effect, indicates a permanent positive axial current flow which exceeds 10 kA within the pinched plasma column. Obviously, this axially flowing pinch

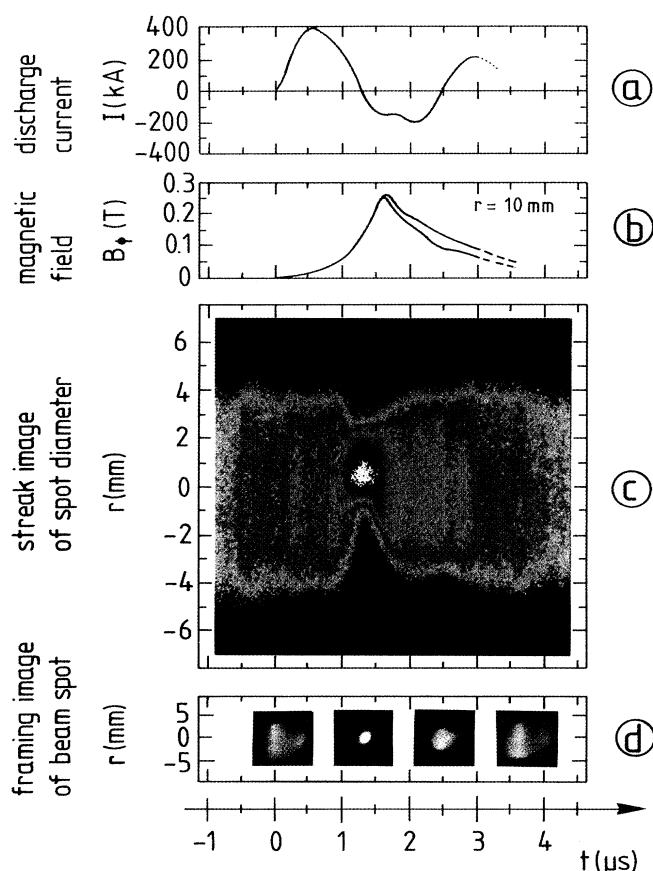


FIG. 2. Presentation of (a) discharge current, (b) magnetic field, (c) streak image, and (d) framing images as a function of time  $t$ . Time zero indicates the start of discharge. The streak image was taken with a  $200\text{-}\mu\text{m}$ -wide slit at 38 cm distance behind the pinch. The exposure time for the framing images was 200 ns with an interframing time of  $1\ \mu\text{s}$ .

current does not follow the alternating discharge current but keeps its original direction, producing the focusing effect for the positive ions. Consequently, this permanent positive axial current has to be compensated by zones with negative current flow further outside of the plasma column. A similar behavior was observed in experiments with the CERN plasma lens. Here, at a discharge current of  $\sim 400\ \text{kA}$  the pinch current is  $\sim 500\ \text{kA}$ . This advantageous behavior, enhancing the focusing power significantly, was explained by the “inverse skin effect.”<sup>17,18</sup>

The  $z$  pinch we used for this experiment was originally designed to produce a very homogeneous plasma target<sup>19,20</sup> for measuring the energy loss of heavy ions penetrating a dense plasma environment.<sup>21,22</sup> The minimum pinch radius coincided with the zero crossing of the discharge current, which helps to minimize any disturbing effects on the beam by the magnetic fields. Nevertheless, it soon became apparent that for the ion beams used the transmission through the plasma was influenced by the discharge; this was attributed to a plasma lens

effect.<sup>23</sup> For an effective plasma lens design, however, the pinch current has to be maximized to achieve sufficiently high magnetic-field gradients. In the CERN antiproton lens, field gradients of several hundred tesla per meter were obtained, whereas in our experiments the measured gradients were about 1 order of magnitude less.

The experimentally observed spot size  $\Delta r$  remains finite due to the finite beam emittance  $\epsilon$  and a variety of aberrations. For a convergence angle  $\delta$  the emittance-limited spot size is approximately  $\Delta r_\epsilon = \epsilon/\delta$ . The main aberration constituents are the chromatic aberration caused by the momentum spread  $\Delta p$  of the beam particles and the spherical aberration caused by radial variations of the focusing strength  $\Delta\kappa$ . For Gaussian beams the sum of independent contributions to the aberration causes changes in the focal distance  $\Delta f$ , and adds like

$$\Delta f = \{[(\partial f/\partial\kappa)\Delta\kappa]^2 + [(\partial f/\partial p)\Delta p]^2 + \dots\}^{1/2}.$$

For a given angle of convergence  $\delta$  the aberration-limited final focus radius  $\Delta r_a$  (“disk of least confusion”) is then given by  $\Delta r_a = \Delta f\delta$ .<sup>24</sup>

The experiment was intended as a proof-of-principle testing of the focusing effect and possibly to allow an estimation of the optical lens properties characterized by the quality of field linearity. While passing through the plasma, the heavy ions change their charge state by ionization and recombination processes and lose energy by Coulomb interaction with the plasma particles. At pinch plasma densities of  $1.5 \times 10^{19}\ \text{cm}^{-3}$  the injected  $\text{Ar}^{11+}$  ions are further stripped to higher charge states within a few mm and hence their magnetic rigidity is reduced. These interaction processes also change the focusing strength  $\kappa$  of the plasma lens and add to aberration. In order to estimate the magnitude of these beam-plasma interactions and to separate them from the lens-related aberration due to deviations from the field linearity, a Monte Carlo code<sup>22</sup> was used. The particle trajectories were calculated for an incident beam of 1000 test particles, taking into account various interaction processes leading to a change of charge state or energy loss. Together with the experimental beam emittance of  $5\pi\ \text{mm mrad}$  the focus diameter was determined for different field distributions. The results of the numerical calculation are compared with the experimental data in Fig. 3. We present one calculation with an ideal, purely linear field and one for a purely quadratic field, both distributions normalized to 0.125 T at 5 mm radius. For the linear field a FWHM focus diameter of 0.4 mm was calculated at a distance of 156 mm behind the pinch, with an angle of convergence of  $\sim 25\ \text{mrad}$ , indicating a mostly emittance-limited spot size. For the quadratic field dependence the diameter almost doubled to 0.7 mm at 163 mm demonstrating the importance of field linearity.

According to the calculations the medium charge of the initial  $\text{Ar}^{11+}$ -ion beam increases during the passage

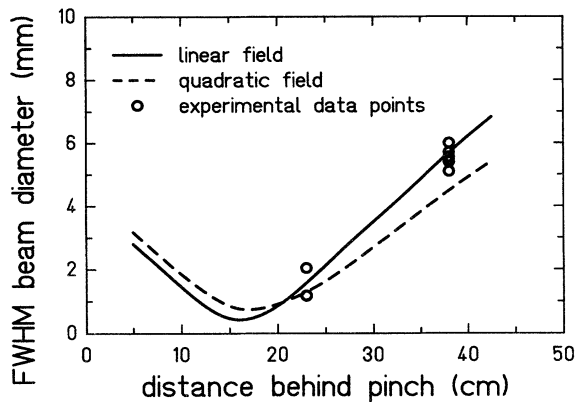


FIG. 3. Comparison of numerical calculations with experimental data taken at the magnetic pinch time of  $1.6 \mu\text{s}$ . The FWHM beam diameter is shown as a function of distance behind the pinch for a linearly rising field  $B_{\phi}(r) = (25 \text{ T/m})r$  with radius  $r$  (solid curve) and a quadratically rising field  $B_{\phi}(r) = (5000 \text{ T/m}^2)r^2$  (dashed curve). Experimental data points at the magnetic pinch time are fitted quite well by the calculated curves.

of the plasma with a density of  $1.5 \times 10^{19} \text{ cm}^{-3}$  to  $\text{Ar}^{17.5+}$  where the ions are equally distributed in charge states  $17+$  and  $18+$ . The corresponding magnetic rigidity reduces from  $\sim 1.8$  to  $\sim 1.1 \text{ Tm}$ , and equally the drift length  $d$  behind the pinch decreases from 286 to 156 mm assuming a constant field gradient of 25 T/m. The calculated energy loss of 18 MeV corresponds to about 4% of the total incident energy.

The measured FWHM beam diameters of 230 and 380 mm are fitted quite well by the calculated curves in Fig. 3. However, it seems difficult to quantitatively determine the degree of linearity of the field distribution. Further time-resolved measurements of the spot size closer to the minimum focal distance at  $\sim 160 \text{ mm}$  are planned. These experiments will be accompanied by more detailed experimental mapping of the magnetic field of the pinch at smaller radii.

In summary, a heavy-ion beam was focused for the first time by a  $z$ -pinch plasma lens. The advantages of this cylindrical wire lens are based on its capability to focus in first order and simultaneously in both transversal planes with negligible absorption, resulting in a symmetric focusing at a short focal length. These characteristics make plasma lenses appear attractive compared to conventional lens devices when extreme focusing power is needed. We consider the development of a fine-focusing plasma lens for focusing of heavy-ion beams from the SIS/ESR facility to sub-mm spot sizes. These beams with a magnetic rigidity of about 6 Tm will need much more focusing power than was possible to obtain with the  $z$  pinch used for this experiment. Further measurements with the present  $z$ -pinch device are scheduled, to perform a thorough investigation of the focusing behavior.

This work was supported by the Bundesministerium

für Forschung und Technologie der Bundesrepublik Deutschland under Contracts No. 06 MM 312 and No. 06 AC 301 I.

<sup>1</sup>B. F. Bayanov, J. N. Petrov, G. I. Sil'vestrov, J. MacLachlan, and G. L. Nicholls, *Nucl. Instrum. Methods Phys. Res.* **190**, 9 (1981).

<sup>2</sup>B. F. Bayanov and G. I. Sil'vestrov, *Zh. Tekh. Fiz.* **48**, 160 (1978) [*Sov. Phys. Tech. Phys.* **23**, 94 (1978)].

<sup>3</sup>S. van der Meer, CERN, Geneva, Report No. 62-16, 1962 (unpublished).

<sup>4</sup>W. K. H. Panofsky and W. R. Baker, *Rev. Sci. Instrum.* **21**, 445 (1950).

<sup>5</sup>E. B. Forsyth, L. M. Lederman, and J. Sunderland, *IEEE Trans. Nucl. Sci.* **12**, 872 (1965).

<sup>6</sup>A. Mankofsky and R. N. Sudan, *Nucl. Fusion* **24**, 827 (1984).

<sup>7</sup>J. Watrous and P. F. Ottinger, *Phys. Fluids B* **1**, 1109 (1984).

<sup>8</sup>M. Murayama, K. Masugata, and K. Yatsui, in *Proceedings of the Seventh International Conference on High-Power Beams, Karlsruhe, Germany, July 1988*, edited by W. Bauer and W. Schmidt (Kernforschungszentrum Karlsruhe, Karlsruhe, 1988), Vol. 1, p. 644.

<sup>9</sup>J. Watrous, P. F. Ottinger, and D. Mosher, *Phys. Fluids B* **2**, 378 (1990).

<sup>10</sup>B. Autin, H. Riege, E. Boggasch, K. Frank, L. DeMenna, and G. Miano, *IEEE Trans. Plasma Sci.* **15**, 226 (1987).

<sup>11</sup>F. Dothan, H. Riege, E. Boggasch, and K. Frank, *J. Appl. Phys.* **62**, 3585 (1987).

<sup>12</sup>J. Jacoby, D. H. H. Hoffmann, R. W. Müller, K. Mahrt-Holt, R. C. Arnold, V. Schneider, and J. Maruhn *Phys. Rev. Lett.* **65**, 2007 (1990).

<sup>13</sup>B. Heimrich, H. Nestle, M. Winkler, D. H. H. Hoffmann, and H. Wollnik, *Nucl. Instrum. Methods Phys. Res., Sect. A* **294**, 602 (1990).

<sup>14</sup>J. Meyer-ter-Vehn, S. Witkowski, R. Bock, D. H. H. Hoffmann, I. Hofmann, R. W. Müller, R. Arnold, and P. Mulser, *Phys. Fluids B* **2**, 1313 (1990).

<sup>15</sup>W. Böttcher, in *Plasma Diagnostics*, edited by Lochte Holtgreven (North-Holland, Amsterdam, 1968), p. 614.

<sup>16</sup>H. Kunze, R. Noll, C. R. Haas, M. Elfers, J. Hertzberg, and G. Herziger, *Laser Part. Beams* (to be published).

<sup>17</sup>M. G. Haines, *Proc. Phys. Soc.* **74**, 576 (1959).

<sup>18</sup>E. Boggasch, dissertation, University of Erlangen, Federal Republic of Germany, 1987 (unpublished).

<sup>19</sup>R. Noll, C. R. Haas, and H. Kunze, *J. Phys. (Paris), Colloq, Suppl. 12*, **49**, C7-177 (1988).

<sup>20</sup>R. Noll, R. Kunze, and C. R. Haas, *Nucl. Instrum. Methods Phys. Res., Sect. A* **278**, 85 (1989).

<sup>21</sup>K.-G. Dietrich, D. H. H. Hoffmann, H. Wahl, C. R. Haas, H. Kunze, W. Brandenburg, and R. Noll, *Z. Phys. D* **16**, 229 (1990).

<sup>22</sup>D. H. H. Hoffmann, K. Weyrich, H. Wahl, D. Gardés, R. Bimbot, and C. Fleurier, *Phys. Rev. A* **42**, 2313 (1990).

<sup>23</sup>D. Gardés, R. Bimbot, S. Della-Negra, M. Dumail, B. Kubica, A. Richard, M. F. Rivet, A. Servajean, C. Fleurier, A. Sanba, C. Deutsch, G. Maynard, D. H. H. Hoffmann, K. Weyrich, and H. Wahl, *Europhys. Lett.* **8**, 701 (1988).

<sup>24</sup>J. D. Lawson, *The Physics of Charged-Particle Beams* (Clarendon, Oxford, 1988).

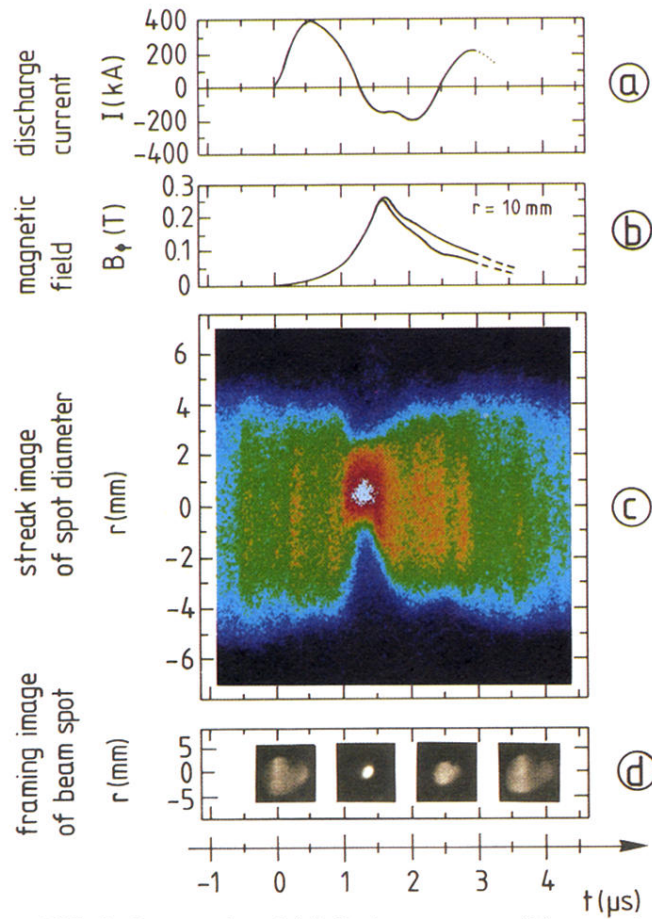


FIG. 2. Presentation of (a) discharge current, (b) magnetic field, (c) streak image, and (d) framing images as a function of time  $t$ . Time zero indicates the start of discharge. The streak image was taken with a  $200\text{-}\mu\text{m}$ -wide slit at 38 cm distance behind the pinch. The exposure time for the framing images was 200 ns with an interframing time of  $1 \mu\text{s}$ .